Direct and Converse Flexoelectricity in Two-Dimensional Materials

Matteo Springolo,[1] Miquel Royo,[1,*] and Massimiliano Stengel[1,2,†]
[1]Institut de Ciència de Materials de Barcelona (ICMAB-CSIC), Campus UAB, 08193 Bellaterra, Spain
[2]ICREA—Institució Catalana de Recerca i Estudis Avançats, 08010 Barcelona, Spain

(Received 16 October 2020; revised 16 July 2021; accepted 30 September 2021; published 19 November 2021)

Building on recent developments in electronic-structure methods, we define and calculate the flexoelectric response of two-dimensional (2D) materials fully from first principles. In particular, we show that the open-circuit voltage response to a flexural deformation is a fundamental linear-response property of the crystal that can be calculated within the primitive unit cell of the flat configuration. Applications to graphene, silicene, phosphorene, boron nitride, and transition-metal dichalcogenide monolayers reveal that two distinct contributions exist, respectively of purely electronic and lattice-mediated nature. Within the former, we identify a key *metric* term, consisting in the quadrupolar moment of the unperturbed charge density. We propose a simple continuum model to connect our findings with the available experimental measurements of the converse flexoelectric effect.

DOI: 10.1103/PhysRevLett.127.216801

Among their many prospective applications, two-dimensional (2D) materials have received, in the past few years, considerable attention as a basis for novel electromechanical device concepts, such as sensors or energy harvesters [1,2]. Such an interest has stimulated intense research, both experimental and theoretical, to characterize the fundamentals of electromechanical couplings in monolayer (or few-layer) graphene [3,4], boron nitride (BN) [5,6], and transition-metal dichalcogenides [1,7]. For the most part, efforts were directed at understanding piezoelectric and piezotronic properties [1] with stretchable and tunable electronics in mind; more recently flexoelectricity has been attracting increasing attention [2,8].

Flexoelectricity, describing the coupling between a strain gradient and the macroscopic polarization [9,10], is expected to play a prominent role in 2D crystals due to their extreme flexibility. Recently, several experimental works [4,7,8] reported a significant out-of-plane electromechanical response in graphene, BN, transition-metal dichalcogenides (TMDs), and related materials. Experiments were generally performed via piezoelectric force microscopy (PFM), which probes the *converse* effect (deformations in response to an applied voltage) in terms of an effective piezoelectric coefficient, d_{33}^{eff}. How the measured values of d_{33}^{eff} relate to the intrinsic flexoelectric coefficients of the 2D layer is, however, currently unknown. First, experiments are usually performed on supported layers [7,8]; this implies a suppression of their mechanical response due to substrate interaction [11], whose impact on d_{33}^{eff} remains poorly understood. Second, flexoelectricity is a nonlocal effect, where electromechanical stresses depend on the *gradients* of the applied external field; this substantially complicates the analysis compared to the piezoelectric case, where spatial inhomogeneities in the tip potential play little role [12]. In fact, even understanding what components of the 2D flexoelectric tensor contribute to d_{33}^{eff} is far from trivial [7]. Unless these questions are settled by establishing reliable models of the converse flexoelectric effect in 2D crystals, the analysis of the experimental data remains to a large extent speculative, which severely limits further progress toward a quantitative understanding.

Theoretical simulations are a natural choice to shed some light on the aforementioned issues. Several groups have studied flexoelectricity in a variety of monolayer crystals including graphene, hexagonal BN, and transition metal dichalcogenides; calculations were performed either from first principles [3,5,13–16] or by means of classical force fields [17,18]. Most authors, however, have defined and calculated the flexoelectric coefficient as a dipolar moment of the deformed layer, which has two main shortcomings. First, calculating the dipole moment of a curved crystalline slab is not free from ambiguities [19], and this has resulted in a remarkable scattering of the reported results. Second, such a definition has limited practical value, unless its relationship with the experimentally relevant parameters (electric fields and potentials) is established. The latter issue may appear insignificant at first sight, but should not be underestimated, as the Poisson equation of electrostatics is modified by curvature in a nontrivial way [20]. Some controversies around the thermodynamic equivalence between the direct and converse flexoelectric effect [21,22] complicate the situation even further, calling for a fundamental solution to the problem. Thanks to the progress of the past few years in the computational methods [20,23–28], addressing these questions in the framework of first-principles linear-response theory appears now well within reach.

Here we overcome the aforementioned limitations by defining and calculating flexoelectricity as the open-circuit voltage response to a flexural deformation ("flexovoltage")

of the 2D crystal in the linear regime. Building on the recently developed implementation of bulk flexoelectricity in 3D [28,29], we show that the flexovoltage coefficient, φ, is a fundamental linear-response property of the crystal and can be calculated by using the primitive 2D cell of the unperturbed flat layer. We demonstrate our method by studying several monolayer materials as testcases (C, Si, P, BN, MoS_2, WSe_2, and SnS_2), which we validate against direct calculation of nanotube structures. We find that the overall response consists in two well-defined contributions, a clamped-ion (CI) and a lattice-mediated (LM) term, in close analogy with the theory of the piezoelectric response [30]. At the CI level, our calculations show a remarkable cancellation between a dipolar linear-response term and a previously overlooked "metric" contribution, which we rationalize in terms of an intuitive toy model of non-interacting neutral spheres [20,25]. We further demonstrate that φ describes both the direct and converse coupling between local curvature and transverse electric fields in an arbitrary geometry, ranging from nanotubes to flexural phonons and rippled layers. Based on this result, we build a quantitatively predictive model of a flexoelectric layer on a substrate, and we use it to discuss recent experimental findings.

The fundamental quantity that we shall address here is the voltage drop across a thin layer due to a flexural deformation, where the latter is measured by the radius of curvature, R. At the leading order, the voltage drop is inversely proportional to R,

$$\Delta V = \frac{\varphi}{R} + O(R^{-2}), \qquad \varphi = \frac{\mu^{2D}}{\epsilon_0}, \tag{1}$$

where φ can also be expressed as a 2D flexoelectric coefficient (in units of charge, describing the *effective* dipole per unit area that is linearly induced by a flexural deformation) divided by the vacuum permittivity, ϵ_0. Our goal is to calculate the constant of proportionality, φ, which we shall refer to as the "flexovoltage" coefficient.

The underlying physical model is that of a nanotube of radius R constructed by bending a flat layer, as illustrated in Fig. 1(a); the voltage drop between the interior and the exterior is then given by Eq. (1). Another obvious example is that of a long-wavelength flexural phonon [see Fig. 1(b)]. Because of rotational invariance, the modulated strain field locally recovers the same pattern as in Fig. 1(a). [See Ref. [20] and Sec. 2.8.2 of Ref. [25].] At the leading order in the wave vector, $\mathbf{q}$, this results in a local jump in the electrostatic potential across the layer of

$$\Delta V(x,y) = \varphi K(x,y), \tag{2}$$

where the local inverse radius of curvature, $K(x,y) = -\nabla^2 u_z(x,y)$, is given by the Laplacian of the vertical displacement field, u_z (Supplemental Material [31]). As we shall see shortly, the effect originates from the distortion of both the electronic cloud and the crystal structure [Fig. 1(c)].

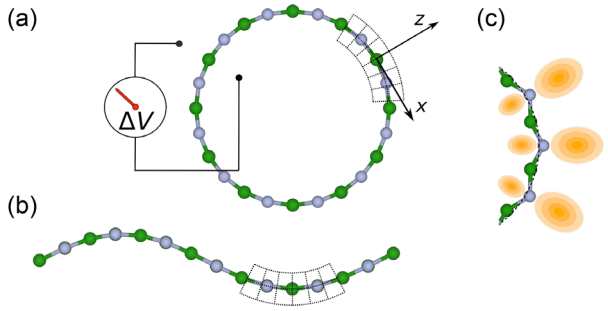

FIG. 1. Schematic illustration of the flexoelectric response in BN. (a) Cross-section of a BN nanotube; the voltage drop between its inner and outer sides is highlighted. (b) Flexural phonon, corresponding to an in-plane modulation of the same strain field as in (a). (c) Lattice-mediated and purely electronic effects contributing to the dipole. Gray and green circles represent the B and N atoms, respectively. The deformed electronic orbitals are shown as yellow shaded ellipses.

To express the flexovoltage as a linear-response property, we start by associating the flexural deformation with a mapping between the Cartesian frame of the flat layer, and the curvilinear frame of the bent nanotube [dashed grid in Fig. 1(a)]. In a neighborhood of the nanotube surface, such a mapping corresponds to a strain field with cylindrical symmetry, of the type $\varepsilon_{xx}(z) = z/R$, where $\hat{z}$ is the normal to the layer surface, $\hat{x}$ runs over the tangential direction, and $\varepsilon_{\alpha\beta}$ is the symmetric strain tensor. This results in a macroscopic transverse strain gradient $\varepsilon_{xx,z} = \partial\varepsilon_{xx}/\partial z = 1/R$, whose amplitude is the inverse radius of curvature [25,42] and will play the role of the perturbative parameter, λ, henceforth.

To discuss the electrostatic potential, which defines the open-circuit voltage φ, we shall frame our arguments on the Poisson equation in the curvilinear frame of the bent layer, following the guidelines of Refs. [20,25,42],

$$\boldsymbol{\nabla} \cdot (\boldsymbol{\epsilon} \cdot \mathbf{E}) = \rho, \qquad \boldsymbol{\epsilon} = \epsilon_0 \sqrt{g}\mathbf{g}^{-1}. \tag{3}$$

The main difference with respect to the Cartesian formulation is that the vacuum permittivity here becomes a tensor that depends on the metric of the deformation, $\mathbf{g}$. Within the linear regime, one can write $\rho = \rho^{(0)} + \lambda\rho^{(1)} + \cdots$, where $\rho^{(0)}$ is the unperturbed density and $\rho^{(1)}$ the first-order response in λ. (For the time being we shall assume that $\rho^{(1)}$ refers to the static response, inclusive of electronic and ionic relaxations.) We find that the open-circuit potential φ is given by

$$\varphi = \frac{\mathcal{D}[\rho^{(1)}]}{\epsilon_0} + \varphi^M, \qquad \varphi^M = -\frac{\mathcal{Q}[\rho^{(0)}]}{2\epsilon_0}, \tag{4}$$

where

$$\mathcal{D}[f] = \int dz\, z f(z) \qquad \mathcal{Q}[f] = \int dz\, z^2 f(z). \quad (5)$$

indicate the first (dipolar) and second (quadrupolar) moment of the function f along the out-of-plane direction z, and $\rho^{(0)}(z)$ and $\rho^{(1)}(z)$ are the in-plane averages of the respective microscopic response functions. $\mathcal{D}[\rho^{(1)}]$ corresponds to the λ-derivative of the "radial polarization" ($\mathbf{p}$) as defined in Ref. [19]; the second term in Eq. (4) is a *metric* contribution that depends only on the unperturbed density $\rho^{(0)}$, and originates from the linear variation of $\boldsymbol{\epsilon}$ in Eq. (3). As we shall see shortly, the dipolar linear-response part is always large and negative, while the metric term is large and positive, typically leading to an almost complete mutual cancellation.

The challenging part of the problem consists in computing the dipolar linear-response contribution. To facilitate our progress toward a practical method, we shall use $\rho^{(1)} = -\nabla \cdot \mathbf{P}^{(1)}$, where $\mathbf{P}^{(1)}$ is the microscopic *polarization* response to the deformation. (The zeroth moment of $P_z^{(1)}$ along z yields $\mathcal{D}[\rho^{(1)}]$, after an integration by parts.) Then, by using the formulation of Ref. [20], we can write the radial component of $\mathbf{P}^{(1)}$ as

$$P_z^{(1)}(z) = z P^U_{z,xx}(z) + P^G_{zz,xx}(z). \quad (6)$$

The cell-periodic response functions $P^U_{z,xx}(z)$ and $P^G_{zz,xx}(z)$ (in-plane averaging is assumed) have the physical interpretation of a *local* piezoelectric (U) and flexoelectric (G) coefficient [42]. The rationale behind such a decomposition is rooted on the availability of efficient first-principles methods to calculate both terms in Eq. (6), as we shall illustrate in the following.

To perform the actual calculations, we shall accommodate the unperturbed (flat) monolayer in a standard supercell, where the out-of-plane dimension L is treated as a convergence parameter. Regarding the gradient (G) contribution, we find

$$\varphi^G = \frac{1}{\epsilon_0} \int dz P^G_{zz,xx}(z) = \frac{L}{\epsilon_0 \epsilon_{zz}} \mu_{zz,xx}, \quad (7)$$

where ϵ_{zz} is the out-of-plane component of the macroscopic dielectric tensor, and $\mu_{zz,xx}$ is the transverse component of the flexoelectric tensor of the supercell. Clearly, both $\mu_{zz,xx}$ and ϵ_{zz} depend on L (averaging over an arbitrary supercell volume is implied, and short-circuit electrical boundary conditions are usually imposed [28] in the calculation of $\boldsymbol{\mu}$). However, they do so in such a way that their ratio multiplied by L does not (assuming that L is large enough to consider the repeated layers as nonoverlapping). Regarding the contribution of the first term on the right-hand side of Eq. (6), we have

$$\varphi^{\mathrm{U}} = \frac{\mathcal{D}[P^U_{z,xx}]}{\epsilon_0} = \frac{\mathcal{Q}[\rho^U_{xx}]}{2\epsilon_0}, \quad (8)$$

where $\rho^U_{xx}(z)$ is the first-order charge-density response to a uniform strain ($\rho^U_{xx} = -\partial P^U_{z,xx}/\partial z$). The total flexovoltage of the slab is then given by

$$\varphi = \frac{dV}{d\lambda} = \varphi^G + \varphi^U + \varphi^M, \quad (9)$$

where neither of φ^G, φ^U or φ^M depend on L, and should therefore be regarded as well-defined physical properties of the isolated monolayer. One can verify that, by applying the present formulation to crystalline slabs of increasing thickness, we recover the results of Ref. [42] once φ is divided by the slab thickness, t, and the thermodynamic limit performed. (φ^G and $\varphi^U + \varphi^M$ tend to the bulk and surface contributions to the total flexoelectric effect, respectively.)

Equation (9) is directly suitable for a numerical implementation, as it requires only response functions that are routinely calculated within density-functional perturbation theory (DFPT). The partition between "G" and "U" contributions, however, is hardly meaningful for an atomically thin 2D monolayer, where essentially everything is surface and there is no bulk underneath. Thus, we shall recast Eq. (9) in a more useful form hereafter, by seeking a separation between CI and LM effects instead [Fig. 1(b)],

$$\varphi = \varphi^{\mathrm{CI}} + \varphi^{\mathrm{LM}}. \quad (10)$$

We find (Supplemental Material [31]) that the CI contribution has the same functional form as the total response,

$$\varphi^{\mathrm{CI}} = \frac{L}{\epsilon_0 \bar{\epsilon}_{zz}} \bar{\mu}_{zz,xx} + \frac{\mathcal{Q}[\bar{\rho}^U_{xx}]}{2\epsilon_0} - \frac{\mathcal{Q}[\rho^{(0)}]}{2\epsilon_0}, \quad (11)$$

with the only difference that the flexoelectric (μ), dielectric (ϵ_{zz}), and uniform-strain charge response (ρ^U) functions have been replaced here with their CI counterparts, indicated by barred symbols. Regarding the LM part,

$$\varphi^{\mathrm{LM}} = \frac{1}{S\epsilon_0} \hat{Z}^{(z)}_{\kappa\alpha} \hat{\Phi}^{-1}_{\kappa\alpha,\kappa'\beta} \hat{C}^{\kappa'}_{\beta z,xx}, \quad (12)$$

we have a more intuitive description in terms of the out-of-plane *longitudinal* charges $\hat{Z}^{(z)}_{\kappa\alpha} = Z^{(z)}_{\kappa\alpha}/\bar{\epsilon}_{zz}$, the pseudoinverse [43] of the zone-center force-constant matrix, $\hat{\Phi}^{-1}_{\kappa\alpha,\kappa'\beta}$, and the atomic force response (Supplemental Material [31]) to a flexural deformation of the slab, $\hat{C}^{\kappa}_{\beta z,xx}$. Note that the "mixed" contribution [24] to the bulk flexoelectric tensor exactly cancels (Supplemental Material [31]) with an equal and opposite term in the LM contribution to φ^U, hence its absence from Eq. (10).

TABLE I. Clamped-ion (CI), lattice-mediated (LM), and total flexovoltages (nV · m) of the 2D crystals studied in this work. Because of its lower symmetry, for phosphorene two independent bending directions (armchair and zigzag) exist.

	φ^{CI}	φ^{LM}	φ
C	−0.1134	0.0000	−0.1134
Si	0.0585	0.0000	0.0585
P (zigzag)	0.2320	−0.0151	0.2170
P (armchair)	−0.0130	−0.0461	−0.0591
BN	−0.0381	−0.1628	−0.2009
MoS_2	−0.2704	−0.0565	−0.3269
WSe_2	−0.3158	−0.0742	−0.3899
SnS_2	0.1864	0.1728	0.3592

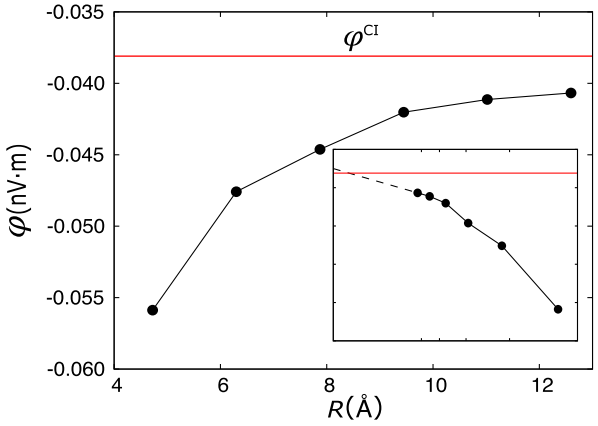

FIG. 2. CI flexovoltage coefficient calculated as $\varphi = \Delta V R$, plotted as a function of the nanotube radius R. Our linear-response result [Eq. (11)] is shown as a red line. The inset shows φ as a function of $1/R$, the dashed line being a linear extrapolation from the last two calculated points to $R \to \infty$.

Our calculations are performed in the framework of DFPT [44,45] within the local-density approximation, as implemented in ABINIT [29,46]. (Computational parameters and extensive tests, including calculations performed within the generalized-gradient approximation, are described in the Supplemental Material [31]). In Table I we report the calculated bending flexovoltages for several monolayer crystals. Both the CI and LM contributions show a considerable variety in magnitude and sign: while the former dominates in the TMDs, the reverse is true for BN, and SnS_2 seems to lie right in the middle. The case of phosphorene is interesting: its lower symmetry allows for a nonzero φ^{LM} in spite of it being an elemental crystal like C and Si; it also allows for a substantial anisotropy of the response. If we assume a physical thickness t corresponding to the bulk interlayer spacing, we obtain an estimate (see Table 6 of the Supplemental Material [31]) for the volume-averaged flexoelectric coefficients, of $|\mu| = |\mu^{2\mathrm{D}}|/t \sim 1$–5 pC/m. ($\mu$, unlike $\mu^{2\mathrm{D}}$, is inappropriate [19] for 2D layers given the ill-defined nature of the parameter t; we use it here for comparison purposes only.) This value is in the same ballpark as earlier predictions [13,15–17], although there is a considerable scatter in the latter. For example, the value quoted by Ref. [17] for graphene is very close to ours, but their results for other materials are either much larger (TMDs, silicene) or much smaller (BN); other works tend to disagree both with our results and among themselves. These large discrepancies are likely due to the specific computational methods that were adopted in each case (often the total dipole moment of a bent nanoribbon including the boundaries was calculated, rather than the intrinsic response of the extended layer), or to the aforementioned difficulties [19] with the definition of the dipole of a curved surface.

Very recently Ref. [19] reported first-principles calculations of some of the materials presented here by using methods that bear some similarities to ours, which allows for a more meaningful comparison. By converting our results for Si and C to the units of Ref. [19] via Eq. (1), we obtain $\mu_{\mathrm{C}} = -0.0063e$ and $\mu_{\mathrm{Si}} = +0.0032e$; these, however, are almost two orders of magnitude smaller, and with inconsistent signs, with respect to the corresponding results of Ref. [19]. We ascribe the source of disagreement to the neglect in Ref. [19] of the metric term in Eq. (11). Indeed, for the dipolar linear-response contribution [first two terms in Eq. (11)] we obtain $\mu_{\mathrm{C}}^{\mathrm{dip}} = -0.22e$ and $\mu_{\mathrm{Si}}^{\mathrm{dip}} = -0.19e$, now in excellent agreement (except for the sign) with the results of Codony *et al.* This observation points to a nearly complete cancellation between the dipolar and metric contribution to φ, which is systematic across the whole materials set (see Table 3 of the Supplemental Material [31]).

To clarify this point, we have performed additional calculations on a toy model, consisting of a hexagonal layer of well-spaced rare gas atoms [31]. This is a system in which no response should occur, as an arbitrary "mechanical deformation" consists in the trivial displacement of noninteracting (and spherically symmetric) neutral atoms. We find that φ^{dip} and φ^{met} are, like in other cases, large and opposite in sign; this, however, is just a side effect of the coordinate transformation (i.e., a mathematical artefact), and does not reflect a true physical response of the system to the perturbation. For a lattice parameter that is large enough, the cancellation becomes exact and our calculated value of φ vanishes as expected on physical grounds. This further corroborates the soundness of our definition of $\mu^{2\mathrm{D}}$, which is based on the electrostatic potential. The latter, in addition to being an experimentally relevant parameter, behaves as a true scalar under a coordinate transformation; it is therefore unaffected, unlike the charge density, by the (arbitrary) choice of the reference frame [31].

As a further consistency check, we have performed explicit calculations of BN nanotubes of increasing radius R, and extracted the voltage drop between their interior and exterior, ΔV, at the clamped-ion level. In Fig. 2 we plot the

estimated flexovoltage, given by $R\Delta V$, as a function of R. The asymptotic convergence to the linear-response value of φ^{CI} is clear, consistent with Eq. (1). The convergence rate, however, appears rather slow: at the largest value of R, corresponding to a nanotube primitive cell of 128 atoms, the deviation from φ^{CI} is still of about 10%. This result highlights the difficulties at calculating flexovoltages in 2D systems by using the direct approach [47]; conversely, our method provides an optimally converged solution within few minutes on a modern workstation, and is ideally suited, e.g., for high-throughput screening applications.

The implications of our findings for the interpretation of the experiments are best discussed in terms of the interaction between the flexural modes of a flat layer and an external, generally inhomogeneous, out-of-plane electric field, $\mathcal{E}_z(x,y)$. In full generality, Eq. (2) leads to the following coupling (energy per unit area),

$$E_{\mathrm{flexo}}(u_z,\mathcal{E}_z)=\mu^{2\mathrm{D}}\mathcal{E}_z\nabla^2 u_z, \tag{13}$$

which reduces to $E_{\mathrm{flexo}}=-q^2\mu^{2\mathrm{D}}\mathcal{E}_z u_z$ for monochromatic fields of the type $A(x,y)=A\,\cos(\mathbf{q}\cdot r)$ $[A=(u_z,\mathcal{E}_z)]$. By deriving E_{flexo} with respect to the displacement u_z we obtain the *converse* flexoelectric effect, in the form of a vertical force per unit area, $\mathcal{F}_z=q^2\mu^{2\mathrm{D}}\mathcal{E}_z$, in response to the field. Explicit first-principles calculations of a BN layer under an applied $\mathcal{E}_z$ (Supplemental Material [31]) nicely confirm this prediction: Eq. (13) is the main source of out-of-plane electromechanical response in this class of materials. Note that the *longitudinal* out-of-plane flexoelectric coefficient of a free-standing layer, which we extract as a by-product of our main calculations, always vanishes (see the Supplemental Material [31]) due to translational invariance and thus cannot contribute to the coupling, contrary to the common belief [7,8].

This allows us to generalize the existing models [48] of supported 2D layers by incorporating flexoelectricity and thereby extract two important messages (Supplemental Material [31]). First, the amplitude of the response is highly sensitive to the substrate interaction strength, g, consistent with the results of recent measurements performed on suspended layers [11]. Second, the response displays a strong dispersion in q, indicating a marked sensitivity on the length scale of the inhomogeneities in the applied field. Both outcomes call for a reinterpretation of the existing PFM measurements of flexoelectricity [7]: information about g and the tip geometry appears essential for a quantitative estimation of $\mu^{2\mathrm{D}}$. We hope that our results will stimulate further experimental research along these lines and more generally to facilitate the design of piezoelectric nanocomposites [49] based on the flexoelectric effect.

We thank Raffaele Resta and Konstantin Shapovalov for their critical read of the manuscript and helpful comments. We acknowledge the support of Ministerio de Economia, Industria y Competitividad (MINECO-Spain) through Grants No. PID2019—108573 GB-C22 and Severo Ochoa FUNFUTURE center of excellence (CEX2019-000917-S) and of Generalitat de Catalunya (Grant No. 2017 SGR1506). This project has received funding from the European Research Council (ERC) under the European Union's Horizon 2020 research and innovation program (Grant Agreement No. 724529). Part of the calculations were performed at the Supercomputing Center of Galicia (CESGA).

*mroyo@icmab.es
†mstengel@icmab.es

[1] W. Wu, L. Wang, Y. Li, F. Zhang, L. Lin, S. Niu, D. Chenet, X. Zhang, Y. Hao, Tony F. Heinz, J. Hone, and Z. L. Wang, Piezoelectricity of single-atomic-layer MoS_2 for energy conversion and piezotronics, Nature (London) **514**, 470 (2014).
[2] F. Ahmadpoor and P. Sharma, Flexoelectricity in two-dimensional crystalline and biological membranes, Nanoscale **7**, 16555 (2015).
[3] S. V. Kalinin and V. Meunier, Electronic flexoelectricity in low-dimensional systems, Phys. Rev. B **77**, 033403 (2008).
[4] L. J. McGilly *et al.*, Visualization of Moiré superlattices, Nat. Nanotechnol. **15**, 580 (2020).
[5] I. Naumov, A. M. Bratkovsky, and V. Ranjan, Unusual Flexoelectric Effect in Two-Dimensional Noncentrosymmetric sp^2-Bonded Crystals, Phys. Rev. Lett. **102**, 217601 (2009).
[6] K.-A. N. Duerloo, M. T. Ong, and E. J. Reed, Intrinsic piezoelectricity in two-dimensional materials, J. Phys. Chem. Lett. **3**, 2871 (2012).
[7] C. J. Brennan, R. Ghosh, K. Koul, S. K. Banerjee, N. Lu, and E. T. Yu, Out-of-plane electromechanical response of monolayer molybdenum disulfide measured by piezoresponse force microscopy, Nano Lett. **17**, 5464 (2017).
[8] C. J. Brennan, K. Koul, N. Lu, and E. T. Yu, Out-of-plane electromechanical coupling in transition metal dichalcogenides, Appl. Phys. Lett. **116**, 053101 (2020).
[9] P. Zubko, G. Catalan, and A. K. Tagantsev, Flexoelectric effect in solids, Annu. Rev. Mater. Res. **43**, 387 (2013).
[10] B. Wang, Y. Gu, S. Zhang, and L.-Q. Chen, Flexoelectricity in solids: Progress, challenges, and perspectives, Prog. Mater. Sci. **106**, 100570 (2019).
[11] X. Wang, A. Cui, F. Chen, L. Xu, Z. Hu, K. Jiang, L. Shang, and J. Chu, Probing effective out-of-plane piezoelectricity in van der waals layered materials induced by flexoelectricity, Small **15**, 1903106 (2019).
[12] T. Jungk, Á. Hoffmann, and E. Soergel, Influence of the inhomogeneous field at the tip on quantitative piezoresponse force microscopy, Appl. Phys. A **86**, 353 (2007).
[13] W. Shi, Y. Guo, Z. Zhang, and W. Guo, Flexoelectricity in monolayer transition metal dichalcogenides, J. Phys. Chem. Lett. **9**, 6841 (2018).
[14] W. Shi, Y. Guo, Z. Zhang, and W. Guo, Strain gradient mediated magnetism and polarization in monolayer VSe_2, J. Phys. Chem. C **123**, 24988 (2019).

[15] T. Pandey, L. Covaci, and F. M. Peeters, Tuning flexoelectricty and electronic properties of zig-zag graphene nanoribbons by functionalization, Carbon **171**, 551 (2021).

[16] T. Pandey, L. Covaci, and M. V. Milošević, and F. M. Peeters, Flexoelectricity and transport properties of phosphorene nanoribbons under mechanical bending, Phys. Rev. B **103**, 235406 (2021).

[17] X. Zhuang, B. He, B. Javvaji, and H. S. Park, Intrinsic bending flexoelectric constants in two-dimensional materials, Phys. Rev. B **99**, 054105 (2019).

[18] B. Javvaji, B. He, X. Zhuang, and H. S. Park, High flexoelectric constants in janus transition-metal dichalcogenides, Phys. Rev. Mater. **3**, 125402 (2019).

[19] D. Codony, I. Arias, and P. Suryanarayana, Transversal flexoelectric coefficient for nanostructures at finite deformations from first principles, Phys. Rev. Mater. **5**, L030801 (2021).

[20] M. Stengel, Microscopic response to inhomogeneous deformations in curvilinear coordinates, Nat. Commun. **4**, 2693 (2013).

[21] L. E. Cross, Flexoelectric effects: Charge separation in insulating solids subjected to elastic strain gradients, J. Mater. Sci. **41**, 53 (2006).

[22] P. V. Yudin and A. K. Tagantsev, Fundamentals of flexoelectricity in solids, Nanotechnology **24**, 432001 (2013).

[23] R. Resta, Towards a Bulk Theory of Flexoelectricity, Phys. Rev. Lett. **105**, 127601 (2010).

[24] M. Stengel, Flexoelectricity from density-functional perturbation theory, Phys. Rev. B **88**, 174106 (2013).

[25] M. Stengel and D. Vanderbilt, First-principles theory of flexoelectricity, in *Flexoelectricity in Solids From Theory to Applications*, edited by A. K. Tagantsev and P. V. Yudin (World Scientific Publishing Co., Singapore, 2016), Chap. 2, pp. 31–110.

[26] C. E. Dreyer, M. Stengel, and D. Vanderbilt, Current-density implementation for calculating flexoelectric coefficients, Phys. Rev. B **98**, 075153 (2018).

[27] A. Schiaffino, C. E. Dreyer, D. Vanderbilt, and M. Stengel, Metric wave approach to flexoelectricity within density functional perturbation theory, Phys. Rev. B **99**, 085107 (2019).

[28] M. Royo and M. Stengel, First-Principles Theory of Spatial Dispersion: Dynamical Quadrupoles and Flexoelectricity, Phys. Rev. X **9**, 021050 (2019).

[29] A. H. Romero *et al.*, Abinit: Overview and focus on selected capabilities, J. Chem. Phys. **152**, 124102 (2020).

[30] R. M. Martin, Piezoelectricity, Phys. Rev. B **5**, 1607 (1972).

[31] See Supplemental Material at http://link.aps.org/supplemental/10.1103/PhysRevLett.127.216801 about theoretical derivations, computational details, and results, which includes Refs. [32–41].

[32] M. Royo, K. R. Hahn, and M. Stengel, Using High Multipolar Orders to Reconstruct the Sound Velocity in Piezoelectrics from Lattice Dynamics, Phys. Rev. Lett. **125**, 217602 (2020).

[33] D. R. Hamann, Optimized norm-conserving vanderbilt pseudopotentials, Phys. Rev. B **88**, 085117 (2013).

[34] M. J. van Setten, M. Giantomassi, E. Bousquet, M. J. Verstraete, D. R. Hamann, X. Gonze, and G.-M. Rignanese, The PseudoDojo: Training and grading a 85 element optimized norm-conserving pseudopotential table, Comput. Phys. Commun. **226**, 39 (2018).

[35] K. S. Novoselov, A. Mishchenko, A. Carvalho, and A. H. Castro Neto, 2d materials and van der waals heterostructures, Science **353**, aac9439 (2016).

[36] N. A. Pike, B. Van Troeye, A. Dewandre, G. Petretto, X. Gonze, G.-M. Rignanese, and M. J. Verstraete, Origin of the counterintuitive dynamic charge in the transition metal dichalcogenides, Phys. Rev. B **95**, 201106 (2017).

[37] J. P. Perdew, K. Burke, and M. Ernzerhof, Generalized Gradient Approximation Made Simple, Phys. Rev. Lett. **77**, 3865 (1996).

[38] D. R. Hamann, K. M. Rabe, and D. Vanderbilt, Generalized-gradient-functional treatment of strain in density-functional perturbation theory, Phys. Rev. B **72**, 033102 (2005).

[39] A. Jain, S. P. Ong, G. Hautier, W. Chen, W. D. Richards, S. Dacek, S. Cholia, D. Gunter, D. Skinner, G. Ceder, and K. A. Persson, The materials project: A materials genome approach to accelerating materials innovation, APL Mater. **1**, 011002 (2013).

[40] M. Royo and M. Stengel, Exact Long-Range Dielectric Screening and Interatomic Force Constants in Quasi-2d Crystals, Phys. Rev. X **11**, 041027 (2021).

[41] S. Kumar and P. Suryanarayana, Bending moduli for forty-four select atomic monolayers from first principles, Nanotechnology **31**, 43LT01 (2020).

[42] M. Stengel, Surface control of flexoelectricity, Phys. Rev. B **90**, 201112(R) (2014).

[43] J. Hong and D. Vanderbilt, First-principles theory and calculation of flexoelectricity, Phys. Rev. B **88**, 174107 (2013).

[44] S. Baroni, S. de Gironcoli, and A. Dal Corso, Phonons and related crystal properties from density-functional perturbation theory, Rev. Mod. Phys. **73**, 515 (2001).

[45] X. Gonze and C. Lee, Dynamical matrices, Born effective charges, dielectric permittivity tensors, and interatomic force constants from density-functional perturbation theory, Phys. Rev. B **55**, 10355 (1997).

[46] X. Gonze *et al.*, ABINIT: First-principles approach to material and nanosystem properties, Comput. Phys. Commun. **180**, 2582 (2009).

[47] D. Bennett, Flexoelectric-like radial polarization of single-walled nanotubes from first-principles, Electron. Struct. **3**, 015001 (2021).

[48] B. Amorim and F. Guinea, Flexural mode of graphene on a substrate, Phys. Rev. B **88**, 115418 (2013).

[49] B. Chu, W. Zhu, N. Li, and L. E. Cross, Flexure mode flexoelectric piezoelectric composites, J. Appl. Phys. **106**, 104109 (2009).